



## Biosorption of hexavalent chromium from aqueous solutions by *Catla catla* scales: Equilibrium and kinetics studies

Kondapalli Srividya, Kaustubha Mohanty\*

Department of Chemical Engineering, Indian Institute of Technology Guwahati, Guwahati 781039, Assam, India

### ARTICLE INFO

#### Article history:

Received 19 May 2009

Received in revised form 24 August 2009

Accepted 25 August 2009

#### Keywords:

Biosorption

Chromium

Heavy metal

Kinetics

Wastewater treatment

### ABSTRACT

In this work the potential of *Catla catla* scales to remove Cr(VI) ions from aqueous solutions was investigated as a function of time, initial Cr(VI) concentration, initial pH, biomass dose and agitation speed. Optimum biosorption conditions were found to be pH 1.0, 0.05 g L<sup>-1</sup> biomass dosage, 200 rpm agitation speed and 180 min equilibrium time. The fitness of biosorption equilibrium data for Freundlich, Langmuir and Dubinin–Radushkevich isotherm models were tested. It was found that Freundlich model was better suitable for biosorption of Cr(VI) ions onto *C. catla* biomass. Three kinetic models viz. the Lagergren first-order and pseudo-second-order and intra-particle diffusion model were used to analyze the biosorption data and the results suggested that the pseudo-second-order model represented the best correlation. FTIR spectrum analysis revealed that O–H, N–H and C–O groups were the leading Cr(VI) binding groups.

© 2009 Elsevier B.V. All rights reserved.

### 1. Introduction

Environmental pollution due to toxic heavy metals in air, soil and water is a major global problem. Heavy metals cannot be degraded or destroyed; hence they are persistent in all parts of the environment. The reduction amount of these metals from effluents to a permissible limit before discharging them into streams and rivers is very important for human health and environment. Chromium is one of such heavy metals which exist in trivalent and hexavalent forms [1]. Cr(VI) is more toxic and highly soluble whereas Cr(III) is less toxic and less soluble. Strong exposure of Cr(VI) causes cancer in digestive tract and lungs and may cause epigastric pain, nausea, vomiting, severe diarrhea and hemorrhage [2]. Therefore, it is essential to remove Cr(VI) from wastewater before disposal. Extensive use of these chromium species are commonly found in many industries such as leather tanning, aluminium productions, dye, electroplating, chromate manufacturing, metal cleaning and processing [3–5].

Conventional methods for removing Cr(VI) ions from wastewater include, physical and physico-chemical treatment technologies such as ion exchange, electro dialysis, membrane filtration, reverse osmosis, chemical precipitation and adsorption [1,6]. The major disadvantages of these conventional treatment methods are high capital investment as well as recurring expenses and incomplete metal removal, generation of toxic sludge or other waste products that require safe disposal. Continuous search for other

effective new treatment methods has directed attention to biosorption, a techno-economical method for removal of heavy metals [7]. The major advantages of this technique are: high efficiency, complete removal of metal ions even at low concentrations, low operating cost, short operation time and improved selectivity for removal of heavy metals from effluent irrespective of toxicity [2,8].

Biosorption which utilizes biological materials as sorbents is an energy-independent method of binding metals to the cell wall of biomass. It is used not only for toxic metal removal but also for the recovery of precious metals such as gold and silver [6,9]. Literature survey reveals that several biological materials such as non living biomass like bark, lignin, peanut hulls as well as living biomass like fungi, bacteria, yeast, moss, aquatic plants and algae, were investigated for the removal of heavy metals [2,7,10–14]. Biosorption utilizes the ability of biological materials to accumulate heavy metals from waste streams by either metabolically mediated or purely physico-chemical pathways of uptake.

In the present work, scales of *Catla catla* (fish) are used as the biosorbent. Huge amounts of these scales are being generated from fish markets everyday and are thrown away as it is. This paper reports the potential of this unexploited biosorbent for removing Cr(VI) from aqueous solution. The influence of various operating parameters such as initial metal concentration, contact time, biosorbent dose, initial pH of solution and agitation speed on the Cr(VI) biosorption were investigated. The Langmuir and Freundlich models were used to fit the equilibrium isotherms. FTIR spectroscopy and SEM was used to find out the various functional groups present on the cell wall of the biosorbent as well to study the surface morphology of biosorbent.

\* Corresponding author. Tel.: +91 361 2582267; fax: +91 361 2582291.  
E-mail address: [kmohanty@iitg.ernet.in](mailto:kmohanty@iitg.ernet.in) (K. Mohanty).

## 2. Materials and methods

### 2.1. Reagents

All the chemicals/reagents used in these studies were of analytical reagent grade and purchased from Merck, Germany; S.D. Fine Chem. Ltd., India and Rankem, India.

### 2.2. Preparation of biosorbent

*C. catla* scales were collected from the fishermen's market located in Amingaon near IIT Guwahati. These scales were washed repeatedly with water to remove adhering dust and soluble impurities from the surface. The fish scales were dried under sun for two days. The dried scales were then converted into fine powder by grinding in a grinder (Bajaj, Model GX7). These fine particles are kept in the oven at 70 °C for 2 h for removing moisture. By using screen seiver the fine powder was then sieved through 100, 120, 150, 200 and 240 μm mesh to obtain biosorbent with homogeneous known particle size. These powdered biosorbent is preserved in airtight polyethylene containers for further use.

### 2.3. Preparation of stock solution

The adsorption capability of the prepared biosorbent toward Cr(VI) was investigated using aqueous solutions. A stock Cr(VI) solution (1000 mg L<sup>-1</sup>) was prepared by dissolving 2.8269 g of K<sub>2</sub>Cr<sub>2</sub>O<sub>7</sub> in 1000 mL deionized water, shaking it for 15 min at 150 rpm to obtain complete dissolution. The stock solution was diluted as required to obtain standard solutions of concentrations ranging between 10 and 100 mg L<sup>-1</sup> concentrations.

### 2.4. Batch sorption experiments

Batch sorption experiments for kinetic studies were conducted in 250 mL conical flasks at natural solution pH (5.85). Dry native biosorbent were thoroughly mixed individually with 100 mL of stock solution with three different concentrations (10, 30 and 50 mg L<sup>-1</sup>) and the suspensions were shaken at room temperature (28 °C) using an incubator shaker (Daihan LabTech Co. Ltd, Model LSI-3016R). Samples of 5 mL were collected from the conical flasks at required time intervals viz. 20, 40, 60, 80, 100, 120, 150, 180, 210 and 240 min and were filtered through Whatman No. 1 filter paper. The filtrates were analyzed for residual chromium concentration in the solution.

The isotherm studies were carried out by varying the initial chromium concentrations from 1 to 100 mg L<sup>-1</sup> at the natural pH of the solution by adding optimum dose of the biosorbent. After shaking the flask up to the equilibrium time, the solution was analyzed for residual chromium concentration. All the data presented in this manuscript are the average of three experimental runs.

### 2.5. Equipments

Cr(VI) in solution was analyzed by UV-spectrophotometer (PerkinElmer, Model Lambda 35). pH of the solution was measured using a pH meter (Eutech Instruments, Model pHTestr 1, 2). SEM micrographs and EDX spectra obtained by using scanning electron microscopy (LEO, Model 1430VP). FTIR analysis used to detect chemical functional groups present on adsorbent surfaces (PerkinElmer, Model Spectrum one FTIR) [2].

### 2.6. Metal uptake

The biosorption equilibrium uptake capacity for each sample was calculated according to mass balance on the metal ion

expressed as,

$$q = \frac{(C_i - C_e)V}{M} \quad (1)$$

where  $q$  is the equilibrium metal uptake capacity (mg g<sup>-1</sup>),  $V$  is the volume of the solution (L) and  $M$  is mass of biosorbent (g),  $C_i$  is the initial metal ion concentration (mg L<sup>-1</sup>) and  $C_e$  is the equilibrium or final metal ion concentration (mg L<sup>-1</sup>) [2].

The extent of sorption in percentage is found from the relation,

$$\text{Sorption (\%)} = \frac{(C_i - C_e)}{C_i} \times 100 \quad (2)$$

## 3. Results and discussion

### 3.1. Biosorption conventional experimental variables

In this section the effect of different experimental variables like solution pH, agitation speed, biosorbent dosage, contact time and initial metal ion concentrations which are conventionally being used to optimize the suitable experimental conditions for the maximum metal uptake by *C. catla* scales is described comprehensively.

The effect of biosorbent dosage on metal uptake and percentage removal of Cr(VI) has been shown in Fig. 1. It indicates that the specific Cr(VI) uptake values decreased with increase in biosorbent dose. Higher uptake at low biosorbent concentrations could be due to an increased metal-to-biosorbent ratio, which decreases upon an increase in dry biomass dose. Further it indicates that the percentage removal of Cr(VI) increases with the increase in biosorbent dose but beyond a certain value the percentage removal reaches a saturation level. This is because of the resistance to mass transfer of Cr(VI) from bulk solution becomes important at high biosorbent dose in the conical flask in which the experiment was conducted [15]. The percentage removal of Cr(VI) increased from 35.06 to 60.89 when the dose was changed from 0.05 to 0.4 g.

To estimate the sorption capacity of the biosorbent, it is important that the experimental solution be allowed significant time to attain equilibrium. Fig. 2 shows the effect of contact time for five different initial concentrations of Cr(VI) (10–50 mg L<sup>-1</sup>) with biosorbent dose (0.05 g) at natural pH of the solution. The figure shows that percentage removal of Cr(VI) adsorption increases with time from 0 to 180 min or more and then becomes almost constant up to the end of the experiment. It can be concluded that the rate of Cr(VI) binding with biosorbent is more at initial stages, which gradually decreases and become almost constant after an optimum period of 180 min [2,3].

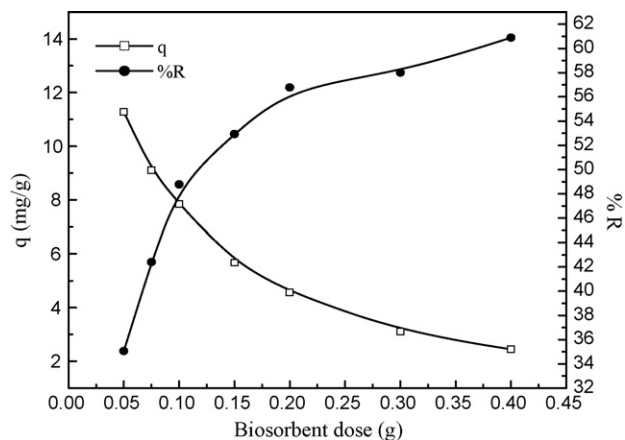


Fig. 1. Effect of biosorbent dose on Cr(VI) biosorption (initial Cr(VI) concentration: 15 mg L<sup>-1</sup>, pH 5.4, contact time: 180 min, agitation speed: 200 rpm, temperature: 28 °C).

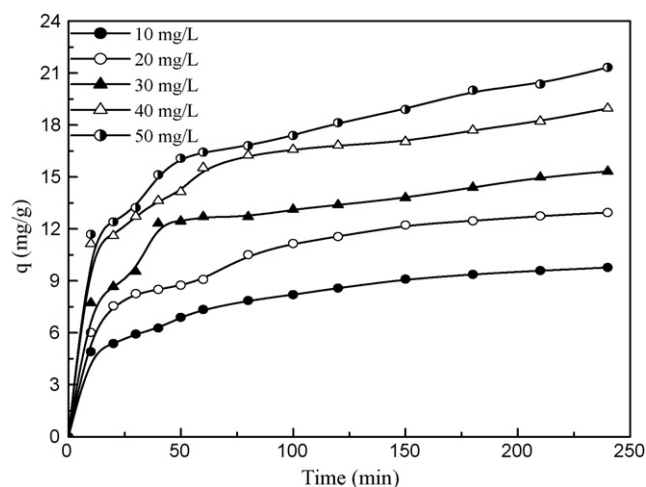


Fig. 2. Effect of contact time on Cr(VI) biosorption (biosorbent dosage: 0.05 g, agitation speed: 200 rpm, pH 5.4, temperature: 28 °C).

Experimental data obtained for the biosorption of Cr(VI) by *C. catla* scales at various Cr(VI) concentrations are represented in Fig. 3. These results revealed that specific Cr(VI) uptake increased with an increase in the initial Cr(VI) concentration. The highest uptake of the biosorbent was around  $21.32 \text{ mg g}^{-1}$  at an Cr(VI) concentration of  $50 \text{ mg L}^{-1}$ . The enhancement in metal sorption could be due to an increase in electrostatic interactions involving the sites of progressively lower affinity for Cr(VI) ions. However, percent adsorption of Cr(VI) decreased from 43% to 20% with an augmentation of Cr(VI) concentration due to rapid saturation of the metal binding sites of the biosorbent [15,16].

Sorption of heavy metals from aqueous solutions depends on properties of biosorbent and transfer of molecules of adsorbate from the solution to the solid phase. pH of the solution is an important parameter that effect the biosorption process. The pH dependence of metal uptake could be related to several functional groups (such as, amino, carboxyl, amide and phosphate etc.) present on the surface of the biosorbent [3]. These groups and their associated ionic states play a dominant role in the extent of biosorption. Biosorbent materials usually have both weak acidic and basic functional groups. It is a well known fact that the binding of heavy metal cations is determined primarily by the state of dissociation of the weak acidic groups. It has also been reported

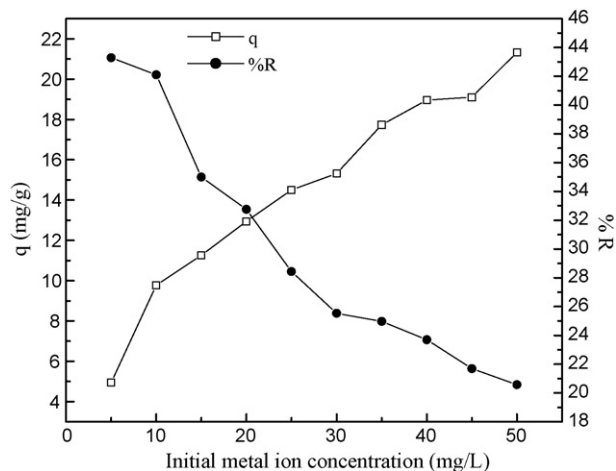


Fig. 3. Effect of initial metal ion concentration on Cr(VI) biosorption (biosorbent dosage: 0.05 g, contact time: 180 min, agitation speed: 200 rpm, pH 5.4, temperature: 28 °C).

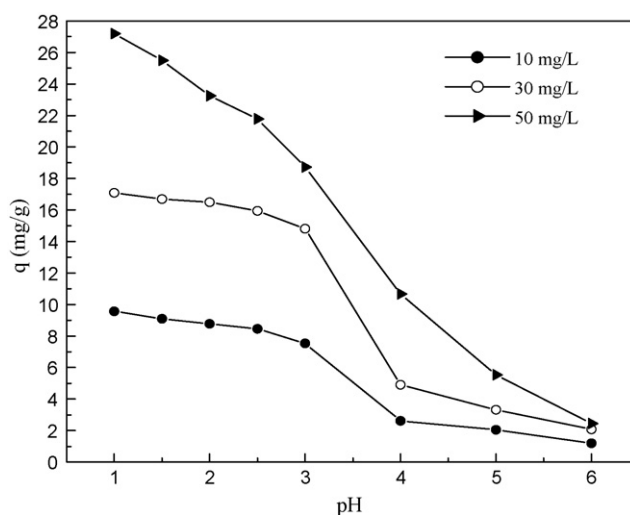


Fig. 4. Effect of pH on Cr(VI) biosorption (biosorbent dosage: 0.05 g, contact time: 180 min, agitation speed: 200 rpm, temperature: 28 °C).

that biosorption capacities for heavy metals are strongly pH sensitive and that the extent of biosorption decreases as solution pH increases [2,5,6,14]. The highest metal uptake was reported to be  $27.18 \text{ mg g}^{-1}$  obtained at pH 1.0 and the overall metal uptake of Cr(VI) decreased to  $2.44 \text{ mg g}^{-1}$  as pH increased up to 6 as shown in Fig. 4. It is important that the maximum biosorption for all concentrations takes place at pH 1.0. This is probably due to the fact that at pH 1.0 the negatively charged chromium species ( $\text{HCrO}_4^-$ ) bind through electrostatic attraction to positively charged functional groups on the surface of biosorbent as at this pH more functional groups carrying a net positive charge would be exposed. But as pH increases, it seems that, the number of functional groups carrying a net negative charge is more, which tends to repulse the anions [4,14]. It is clear from the figure that Cr(VI) is also removed at other pH values, but the rate of the removal is quite slow. Hence, it can be concluded that beyond pH 1.0, other mechanisms like physical adsorption could have taken an important role and ion exchange mechanism might have reduced [2,17].

Agitation speed also plays an important role in the mass transfer of Cr(VI) from the solution to the surface of biosorbent. The biosorption capability of *C. catla* scales for removing Cr(VI) of three different concentrations (10, 30 and  $50 \text{ mg L}^{-1}$ ) at different rpm (50–300) is shown in Fig. 5. Cr(VI) uptake increases with the increase in agitation speed ( $q = 13.64 \text{ mg g}^{-1}$  at 50 rpm and  $40.34 \text{ mg g}^{-1}$  at 300 rpm for  $50 \text{ mg L}^{-1}$  initial Cr(VI) concentration) for a contact time of 3 h. This is due to the fact that with increase in agitation speed, the rate of diffusion of Cr(VI) ions towards the surface of the biosorbent increases [15]. Since the uptake of Cr(VI) beyond 200 rpm was found to be more or less same, so 200 rpm was selected as the optimum agitation speed for all the experiments.

### 3.2. Biosorption kinetics

Kinetics is one of the major parameters to evaluate biosorption dynamics. In order to examine the controlling mechanism of biosorption process such as mass transfer and/or chemical reaction various kinetic models were used. The following mathematical relation between contact time and percent removal has been used to find biosorption kinetics constant for *C. catla* scales [2,17]:

$$R = a(t)^b \quad (3)$$

where,  $R$  is percent removal of Cr(VI),  $a$  and  $b$  are the constants and  $t$  is the contact time in minutes.

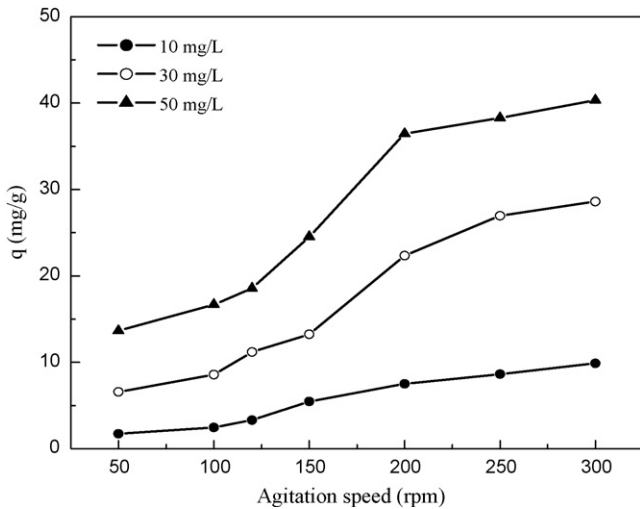


**Fig. 5.** Effect of agitation speed on the Cr(VI) biosorption (biosorbent dosage: 0.05 g, contact time: 180 min, pH 5.4, temperature: 28 °C).

**Table 1**  
Adsorption kinetic constants.

Initial Cr(VI) concentration (mg L <sup>-1</sup> )	Dose (g × 10 <sup>-2</sup> mL <sup>-1</sup> )	<i>a</i>	<i>b</i>
10	0.05	2.24	0.2365
	0.1	3.49	0.2247
30	0.05	2.61	0.2115
	0.1	3.75	0.2006
50	0.05	2.91	0.1905
	0.1	3.88	0.1864

The linearized relationship can be expressed as:

$$\log R = \log a + b \log t \quad (4)$$

By using Eq. (4) constants *a* and *b* were calculated for three different initial Cr(VI) concentrations and the values are shown in Table 1. The values of *a* ranges from 2.24 to 3.88. It is clear from the table that with increase in sorbent dose for same initial Cr(VI) concentration, value of *a* increases, which suggest that with increase in sorbent dose, biosorption capacity also increases. The value of *a* is highest at Cr(VI) concentration of 50 mg L<sup>-1</sup> with a sorbent dose of 0.1 g/100 mL. The value of *b* ranges from 0.1864 to 0.2365. The low values of *b* suggest that with increase in time, the rates of percentage removal of Cr(VI) decreases.

In many cases, the kinetics of biosorption by any biological material has been tested for the first-order expression given by Lagergren. However, it has also been shown that a pseudo-second-order approach can sometimes provide a better description of the biosorption kinetics. The pseudo-first-order kinetic model assumes that “metal sorption process is first-order in nature as it is only dependent on the number of metal ions present at the specific

time in the solution” [18]. In contrast to pseudo-first-order kinetic model, the pseudo-second-order kinetic model assumes that “the metal biosorption process is dependent on the number of metal ions present in the solution as well as the free biosorption sites on the biosorbent surface” [19].

The pseudo-first-order Lagergren model is expressed as:

$$\log(q_e - q) = \log q_e - \left( \frac{K_d}{2.303} \right) t \quad (5)$$

where  $q_e$  is the mass of metal adsorbed at equilibrium (mg g<sup>-1</sup>),  $q_t$  the mass of metal at time  $t$  (min) and  $K_d$  the first-order reaction rate constant of biosorption (min<sup>-1</sup>).

The pseudo-second-order equation is:

$$\frac{t}{q_t} = \left[ \frac{1}{2} K' q_e^2 \right] + \frac{t}{q_e} \quad (6)$$

where  $q_e$  is the mass of metal adsorbed at equilibrium (mg g<sup>-1</sup>),  $q_t$  the mass of metal at time  $t$  (min) and  $K'$  the pseudo-second-order rate constant of biosorption (mg g<sup>-1</sup> min<sup>-1</sup>).

For calculating these rate constants, Lagergren equation as well as the pseudo-second-order equation is plotted (not shown here) for five different concentrations of Cr(VI) with a fixed biosorbent dose. The values of the reaction rate constants and correlation coefficients are listed in Table 2. A comparison between the pseudo-first-order and pseudo-second-order kinetic rate constants suggest that biosorption of Cr(VI) by *C. catla* scales followed closely the pseudo-second-order kinetics rather than the pseudo-first-order kinetics. This is clear from Table 2, since the values of  $q_e$  obtained from pseudo-second-order kinetic equation was close to the experimental  $q_e$  value, whereas that of pseudo-first-order  $q_e$  value did not agree with the experimental value.

In many cases there is a possibility that intra-particle diffusion will be the rate limiting step and this normally determined by using the equation described by Weber and Morris [20]:

$$K_p = \frac{q}{t^{0.5}} \quad (7)$$

where  $q$  (mg g<sup>-1</sup>) is the amount adsorbed at time  $t$  and  $K_p$  is the intra-particle rate constant (mg g<sup>-1</sup> min<sup>-0.5</sup>). To find out the rate constant, Weber and Morris equation is plotted (not shown here) for five different concentrations of Cr(VI) with a fixed biosorbent dose. It is clear that the relationships for *C. catla* scales and Cr(VI) for different concentrations at a particular sorbent dose are not linear over the entire time range, indicating that more than one process is affecting the biosorption [2,21]. The slope of the initial linear portion has been used to derive the intra-particle rate constant,  $K_p$ . The various values of  $K_p$  along with the values of  $q_e$  are shown in Table 2. The rate constant for intra-particle diffusion increased with increasing Cr(VI) concentration. The  $q_e$  values are closer to the experimental values, however in comparison the pseudo-second-order kinetic equation was best fitted.

**Table 2**  
The pseudo-first-order Lagergren and pseudo-second-order constants and Weber and Morris constants.

Initial Cr(VI) concentration (mg L <sup>-1</sup> )	Experimental value	Pseudo-first-order			Pseudo-second-order			Weber and Morris		
		$q_e$ (mg g <sup>-1</sup> )	$K_d$ (min <sup>-1</sup> )	$r^2$	$q_e$ (mg g <sup>-1</sup> )	$K'$ (mg g <sup>-1</sup> min <sup>-1</sup> )	$r^2$	$q_e$ (mg g <sup>-1</sup> )	$K_p$ (mg g <sup>-1</sup> min <sup>-0.5</sup> )	$r^2$
10	9.7758	2.2378	0.0156	0.9866	10.5485	0.0040	0.9966	8.2034	0.4615	0.9441
20	12.9425	2.5841	0.0168	0.9834	14.0647	0.0030	0.9953	11.1563	0.6828	0.9252
30	15.3206	2.3605	0.0126	0.9085	15.9235	0.0037	0.9961	13.1206	0.6687	0.9017
40	18.9586	2.4828	0.0112	0.9671	19.5312	0.0032	0.9968	16.5758	0.649	0.9164
50	21.3275	2.7848	0.0110	0.9781	22.1238	0.0023	0.9939	17.3896	0.7943	0.9399

**Table 3**  
Different isotherm models.

Model	Equation	Reference
Langmuir	$q_e = \frac{q_m K_L C_e}{1 + K_L C_e}$ (8)	Langmuir [23]
	$R_L = \frac{1}{1 + K_L C_0}$ (9)	
Freundlich	$q_e = K_F C_e^{1/n}$ (10)	Freundlich [24]
Dubinin–Radushkevich	$q_e = q_m \exp(-Be^2)$ (11)	Hobson [25]
	$e = RT \ln \left( 1 + \frac{1}{C_e} \right)$ (12)	
	$E = \frac{1}{\sqrt{2B}}$ (13)	

### 3.3. Adsorption isotherms

Analysis of equilibrium sorption data is important for optimizing the design of sorption systems. The equilibrium of biosorption of heavy metals is modeled using adsorption-type isotherms [22]. Adsorption isotherm expresses the relationship between mass of adsorbate per unit weight of adsorbent and liquid phase concentration of adsorbate and provide important design data for adsorption systems. Several sorption isotherm models have been widely used for the equilibrium modeling of biosorption systems. In the present work, two-parameter models, i.e. Langmuir, Freundlich and Dubinin–Radushkevich (D–R) isotherms (Table 3) were used to describe the equilibrium between the Cr(VI) sorbed onto the biomass of *C. catla* scales and Cr(VI) in the solution. The isotherm constants, correlation coefficient ( $r^2$ ) of these models for sorption of Cr(VI) onto *C. Catla* scales for two different temperatures are presented in Table 4.

The Langmuir isotherm model assumes that the uptake of metal ions occurs on a homogeneous surface by monolayer adsorption without any interaction between adsorbed ions [23]. The model further assumes that the energy is same for all active sites of adsorption and there is no interaction between adsorbed ions. In Eq. (8)  $q_e$  is the equilibrium metal ion concentration on the biosorbent ( $\text{mg g}^{-1}$ ),  $C_e$  is the equilibrium metal ion concentration in the solution ( $\text{mg L}^{-1}$ ),  $q_m$  is the monolayer biosorption capacity of the biosorbent ( $\text{mg g}^{-1}$ ), and  $K_L$  is the Langmuir biosorption constant ( $\text{L mg}^{-1}$ ) relating the free energy of biosorption. The Langmuir isotherm model fitted better to the experimental sorption data at temperature  $40^\circ\text{C}$  ( $r^2 = 0.9974$ ) than that at temperature  $20^\circ\text{C}$  ( $r^2 = 0.9923$ ). However, the value of  $q_m$  was increased from 5.05 to  $6.48 \text{ mg g}^{-1}$  with the increase in temperature from 20 to  $40^\circ\text{C}$ , which can be attributed to a rise in kinetic energy of sorbent particles due to the rise in temperature. This rise in kinetic energy increases the frequency of collision between sorbent and sorbate and results in enhanced sorption on to the surface of the sorbent [22].

The essential characteristics of Langmuir isotherm can be explained in terms of dimensionless constant separation factor,  $R_L$

(Eq. (9); Table 3), in which  $K_L$  is the Langmuir constant ( $\text{L mg}^{-1}$ ) and  $C_0$  ( $\text{mg L}^{-1}$ ) is the initial concentration of Cr(VI). According to the value of separation factor  $R_L$ , following types of adsorption exists: (1) favorable adsorption  $0 < R_L < 1$ ; (2) unfavorable adsorption,  $R_L > 1$ ; (3) linear adsorption,  $R_L = 1$  and (4) irreversible adsorption,  $R_L = 0$ .  $R_L$  is a positive number whose magnitude determines the feasibility of the adsorption process [4]. The values of  $R_L$  for both the temperatures are between 0 and 1, indicating favorable biosorption of Cr(VI) onto the scales of *C. catla*.

The Freundlich isotherm model assumes that the uptake of metal ions occurs on a heterogeneous surface by multilayer adsorption and that the amount of adsorbate adsorbed increases infinitely with an increase in concentration [24]. The Freundlich model is empirical in nature which further assumes that the stronger binding sites are occupied first and that the binding strength decreases with increasing degree of site occupation [22]. In Eq. (10),  $q_e$  is the equilibrium metal ion concentration on the biosorbent ( $\text{mg g}^{-1}$ ),  $C_e$  is the equilibrium metal ion concentration in the solution ( $\text{mg L}^{-1}$ ),  $K_F$  and  $1/n$  are the Freundlich model constants related to adsorption capacity and intensity of adsorption, respectively. The values of  $K_F$  and  $1/n$  were found to be 1.13, 0.34 and 2.31, 0.24 at  $20^\circ\text{C}$  and  $40^\circ\text{C}$  respectively. The  $1/n$  values were between 0 and 1, indicating that the biosorption of Cr(VI) onto the scales of *C. catla* is favorable at studied conditions. The Freundlich models fitted the equilibrium biosorption data better than the Langmuir model due to higher value of correlation coefficients (Table 4). Thus, the results of the present study indicate that biosorption of Cr(VI) onto the scales of *C. catla* is heterogeneous in nature.

The sorption data was also subjected to Dubinin–Radushkevich model [25] represented in Eq. (11) where  $q_m$  is the theoretical saturation capacity ( $\text{mg g}^{-1}$ ),  $B$  is a constant related to adsorption energy ( $\text{mol}^2 \text{kJ}^{-2}$ ),  $e$  is the Polanyi potential,  $R$  is the gas constant ( $\text{kJ mol}^{-1} \text{K}^{-1}$ ) and  $T$  is the temperature (K). The D–R isotherm model fitted the equilibrium biosorption data at both the temperatures, however the correlation coefficients were found to be lower than that of Freundlich model. The constant  $B$  gives an idea about the mean free energy  $E$  ( $\text{kJ mol}^{-1}$ ) of adsorption per molecule of adsorbate and can be calculated from D–R isotherm constant  $B$

**Table 4**  
Langmuir, Freundlich and D–R model constants at two different temperatures.

Langmuir isotherm model			Freundlich isotherm model			D–R isotherm model		
Parameters	Values		Parameters	Values		Parameters	Values	
	20 °C	40 °C		20 °C	40 °C		20 °C	40 °C
$r^2$	0.9923	0.9974	$r^2$	0.9992	0.9917	$r^2$	0.9346	0.9615
$q_m$ ( $\text{mg g}^{-1}$ )	5.0581	6.485	$1/n$	0.3419	0.2403	$q_m$ ( $\text{mg g}^{-1}$ )	4.1086	5.699
$K_L$ ( $\text{L mg}^{-1}$ )	0.0943	0.1618	$K_F$ ( $\text{L g}^{-1}$ )	1.1325	2.3147	$B$ ( $\text{kJ}^2 \text{mol}^{-2}$ )	0.0099	0.0055
$R_L$	0.5145	0.4385				$E$ ( $\text{kJ mol}^{-1}$ )	7.0998	9.4728

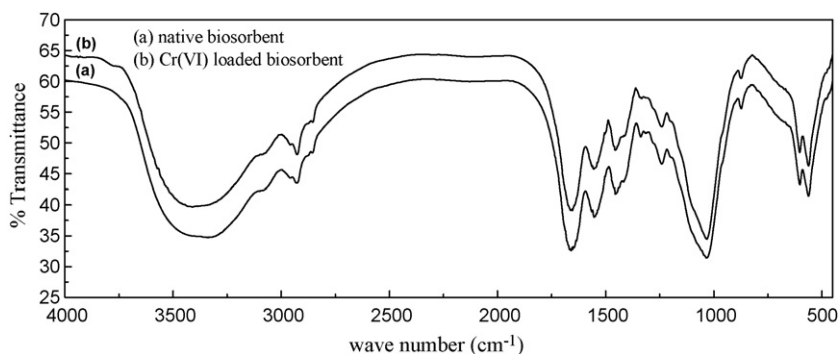


Fig. 6. FTIR spectra of *Catla catla* scales before and after Cr(VI) adsorption.

using Eq. (13). The mean free energy of biosorption gives an idea about biosorption mechanism, whether physical or chemical [5,8]. If the value of  $E$  lies between  $8$  to  $16 \text{ kJ mol}^{-1}$ , the biosorption process takes place chemically and if the value of  $E$  is less than  $8 \text{ kJ mol}^{-1}$ , then the biosorption process takes place physically. In the present study, the value of  $E$  at  $20^\circ\text{C}$  is less than  $8 \text{ kJ mol}^{-1}$ , whereas that at  $40^\circ\text{C}$  is above  $8 \text{ kJ mol}^{-1}$ . This suggests that at low temperature physical adsorption is the dominant process involved and with increase in temperature chemical ion exchange mechanism could have taken an important role.

### 3.4. Fourier transform infrared (FTIR) analysis

Various researchers have suggested that different chemical functional groups such as carboxyl, hydroxyl, amide etc. are responsible for biosorption of metal ions [1,3,5,6,15]. These functional groups are the potential sites for adsorption and the uptake of metal depends on various factors such as abundance of sites, their accessibility, chemical state and affinity between the adsorption site and metal. The FTIR Spectroscopy is an important analytical technique which detects the vibration characteristics of chemical functional

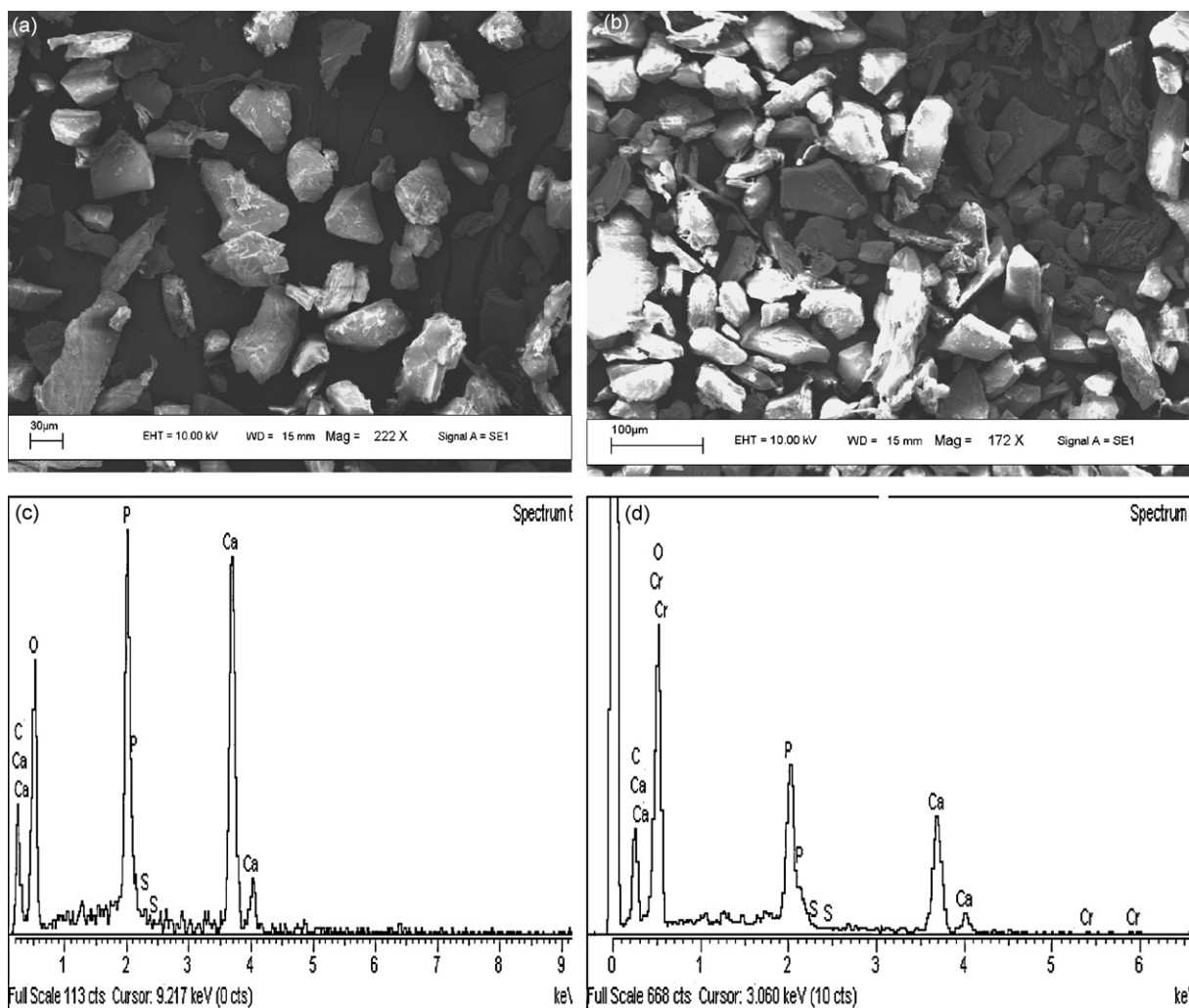


Fig. 7. SEM micrographs of *Catla catla* scales (a) native biosorbent, (b) Cr(VI) loaded biosorbent; EDX spectra of (c) native biosorbent, (d) Cr(VI) loaded biosorbent.

**Table 5**  
Biosorption capacity of Cr(VI) by various biosorbents.

Biosorbent	Initial Cr(VI) concentration (mg L <sup>-1</sup> )	Biosorption capacity (mg g <sup>-1</sup> )	References
<i>Rhizopus nigrificans</i>	50–500	123.45	Sudha and Abraham [12]
Alligator weed	160–360	82.57	Wang et al. [14]
<i>Rhizopus arrhizus</i>	125	8.40	Nourbakhsh et al. [10]
<i>Aeromonas caviae</i>	5–350	69.95	Loukidou et al. [13]
<i>Ceramium virgatum</i>	10	26.5	Sari and Tuzen [8]
<i>Chlorella vulgaris</i>	25–250	24	Veglio and Beolchini [7]
<i>Zoogloea ramigera</i>	25–400	3	Veglio and Beolchini [7]
<i>Neurospora crassa</i>	250	15.85	Tunali et al. [6]
<i>Aspergillus niger</i>	400	117.33	Khambhaty et al. [22]
<i>Rhizopus arrhizus</i>	25–400	62	Prakasham et al. [11]
<i>Clodophara crispata</i>	200	6.20	Nourbakhsh et al. [10]
<i>Lentinus sajor-caju</i>	100	25.2	Arica and Bayramoglu [3]
<i>Saccharomyces cerevisiae</i>	100	4.30	Nourbakhsh et al. [10]
<i>Halimeda oputia</i>	25–400	40	Veglio and Beolchini [7]
<i>Agaricus bisporus</i>	50–125	8.00	Ertugay and Bayhan [4]
Green algae <i>Spirogyra</i> species	5	14.7	Gupta et al. [17]
<i>Eichhornia crassipes</i>	10–30	6.985	Mohanty et al. [2]
<i>Catla catla</i> scales	50	27.18	Present study

groups present on adsorbent surfaces. The adsorbents spectra were measured within the range of 400–4000 cm<sup>-1</sup> wave number. FTIR spectra of both the adsorbents (native as well as chromium loaded) are shown in Fig. 6.

FTIR spectra of native *C. catla* scales (Fig. 6a) show peaks between the region 3500 and 3200 cm<sup>-1</sup> which represented the overlapping peaks of stretching vibration of O–H and N–H groups. The region between 3000 and 2800 cm<sup>-1</sup> exhibited the C–H stretching vibrations of –CH<sub>3</sub> and –CH<sub>2</sub> functional group. Distinct peaks observed between 1730 and 1640 cm<sup>-1</sup> characterize carbonyl groups stretching from aldehydes and ketones. 1300–1470 cm<sup>-1</sup> was the deformation stretching of C–H, –CH<sub>3</sub>, and –CH<sub>2</sub> functional groups. The peaks produced from 3000 to 2500 cm<sup>-1</sup> are due to carboxylic group. The strong band within 1100–1000 cm<sup>-1</sup> is due to C–O group, which is the characteristic peak for polysaccharides. The characteristic band region at 800–850 cm<sup>-1</sup> suggests the presence of sulphonate group in the biomass. The sharp peak observed at lower wave number is due to C–X group, which suggests the presence of various – alkanes groups [15,26].

Changes in intensity and shift in position of the peaks could be observed in FTIR spectrum after Cr(VI) adsorption on *C. catla* scales (Fig. 6b). The first change was the enhancement of the intensity at the region 3500–3200 cm<sup>-1</sup>, indicating an increase of the free hydroxyl group on the biomass. The shifting of peak at 1661 to 1654 cm<sup>-1</sup> indicates that the involvement of N–H of amines and C–O of amides in the adsorption process. The minor shift of the peak from 1034 to 1032 cm<sup>-1</sup> also suggests the involvement of C–O group in binding Cr(VI). It is clear from the FTIR analysis that the possible mechanism of adsorption of Cr(VI) on *C. catla* scales may be due to physical adsorption, ion exchange, surface precipitation, complexation with functional groups and chemical reactions with surface sites [5].

### 3.5. SEM and EDX analysis

Scanning electron microscopy along with energy dispersive X-ray analysis has been used by many researchers for the characterization of the biosorbent as well as elucidation of the probable mechanism of biosorption. SEM micrographs and EDX spectra obtained for native as well as chromium loaded biosorbent are presented in Fig. 6. *C. catla* scales as seen in the micrograph (Fig. 7) are characterized by having two regions, one being white and the other being darker. The white region is rich in inorganic material containing high proportions of calcium and phosphorus whereas the dark region is rich in proteins, because it has a high proportion of carbon, oxygen, and sulphur [27]. Fig. 7b represents the micrograph

of chromium loaded biosorbent. This micrograph clearly shows the presence of new shiny bulky particles over the surface of chromium loaded biosorbent which are absent in the native biosorbent [6]. EDX analysis provides elemental information through analysis of X-ray emissions caused by a high-energy electron beam. The spectra obtained for the native as well as chromium loaded biosorbent (Fig. 7c) indicates the presence of C, Ca, O, P and S. These signals are probably due to the X-ray emissions of proteins and polysaccharides present on the cell wall of the biosorbent [26]. EDX spectra presented in Fig. 7d revealed the additional chromium signal, which confirms the binding of the metal ion to the surface of the biosorbent.

### 3.6. Comparison with other biosorbents

Biosorption capacities of various biosorbents towards Cr(VI) as reported in literature are summarized in Table 5. From the present study it was found that the maximum Cr(VI) uptake by *C. catla* scales for an initial Cr(VI) concentration of 50 mg L<sup>-1</sup> at optimum pH was 27.18 mg g<sup>-1</sup>. The uptake values obtained for Cr(VI) biosorption in this study are comparable and was found to be higher than many other biosorbents. The economic success of any biosorption process depends largely on the cost of biosorbent used. In the present study, the biosorbent that is used is a thrown away material collected from local fish market. Especially in the eastern and southern part of India, due to large consumption of fish, huge amounts of fish scales are being generated everyday. The cost of such scales are absolutely 'zero' and also by adding the cost of drying, grinding, packing and transportation, the cost is very low compared to ion exchange resins [14]. The results thus indicates that *C. catla* scales appears to be cheap as well as efficient biosorbent for the removal of Cr(VI) from aqueous solutions.

## 4. Conclusion

The present study has revealed that *C. catla* scales were efficient in removing hexavalent chromium from aqueous solutions. The sorption process was found to depend on the pH of the solution, pH 1.0 being the optimum value. Increase in the amount of biosorbent increased the percent removal of the metal ions. Kinetic examination of the equilibrium data showed that the biosorption of Cr(VI) onto *C. catla* scales followed well the pseudo-second-order kinetic model. The present results demonstrate that the Freundlich model fits better than the Langmuir as well as D–R model the biosorption equilibrium data in the examined concentration range. FTIR and SEM characterization of the biosorbents has shown a clear

difference in the native and Cr(VI) loaded biosorbents. Based on all results, it can be concluded that *C. catla* scales are an effective and alternative biosorbent for the removal of hexavalent chromium from aqueous solutions because of their considerable biosorption capacity, as well as low-cost. The data so obtained in this study, can be used by various process industries generating low concentrations of hexavalent chromium in wastewater, where using standard adsorbent materials such as ion exchange resins and activated carbons is not economically feasible.

## References

- [1] X. Han, Y.S. Wong, M.H. Wong, N.F.Y. Tama, Biosorption and bioreduction of Cr(VI) by a microalgal isolate *Chlorella miniata*, J. Hazard. Mater. 146 (2007) 65–72.
- [2] K. Mohanty, M. Jha, B.C. Meikap, M.N. Biswas, Biosorption of Cr(VI) from aqueous solutions by *Eichhornia crassipes*, Chem. Eng. J. 117 (2006) 71–77.
- [3] M.Y. Arica, G. Bayramoglu, Cr(VI) biosorption from aqueous solutions using free and immobilized biomass of *Lentinus sajor-caju*: Preparation and kinetic characterization, Colloids Surf. A: Physicochem. Eng. Aspects 253 (2005) 203–211.
- [4] N. Ertugay, Y.K. Bayhan, Biosorption of Cr (VI) from aqueous solutions by biomass of *Agaricus bisporus*, J. Hazard. Mater. 154 (2008) 432–439.
- [5] M. Jain, V.K. Garg, K. Kadirvelu, Chromium(VI) removal from aqueous system using *Helianthus annuus* (sunflower) stem waste, J. Hazard. Mater. 162 (2009) 365–372.
- [6] S. Tunali, K. Ismail, T. Akar, Chromium(VI) biosorption characteristics of *Neurospora crassa* fungal biomass, Miner. Eng. 18 (2005) 681–689.
- [7] F. Veglio, F. Beolchini, Removal of metals by biosorption: a review, Hydrometallurgy 44 (1997) 301–316.
- [8] A. Sari, M. Tuzen, Biosorption of total chromium from aqueous solution by red algae (*Ceramium virgatum*): Equilibrium, kinetic and thermodynamic studies, J. Hazard. Mater. 160 (2008) 349–355.
- [9] B. Volesky, Advances in biosorption of metals. Selection of biomass types, FEMS Microbiol. Rev. 14 (1994) 291–302.
- [10] M. Nourbakhsh, Y. Sag, D. Ozer, Z. Aksu, T. Kutsal, A. Caglar, A comparative study of various biosorbents for removal of chromium(VI) ions from industrial waste waters, Process Biochem. 29 (1994) 1–5.
- [11] R.S. Prakasham, J. Sheno Merrie, R. Sheela, N. Saswathi, S.V. Ramakrishna, Biosorption of chromium(VI) by free and immobilized *Rhizopus arrhizus*, Environ. Pollut. 104 (1999) 421–427.
- [12] B.R. Sudha, T.E. Abraham, Studies on enhancement of Cr (VI) biosorption by chemically modified biomass of *Rhizopus nigricans*, Water Res. 36 (2002) 1224–1236.
- [13] M.X. Loukidou, A.I. Zouboulis, T.D. Karapantsios, K.A. Matis, Equilibrium and kinetic modeling of chromium(VI) biosorption by *Aeromonas caviae*, Colloids Surf. A: Physicochem. Eng. Aspects 242 (2004) 93–104.
- [14] X.S. Wang, Y.P. Tang, R.T. Sheng, Kinetics, equilibrium and thermo dynamics study on removal of Cr(VI) from aqueous solutions using low cost adsorbent Alligator weed, Chem. Eng. J. 148 (2008) 217–225.
- [15] R. Nadeem, T.M. Ansari, A.M. Khalid, Fourier transform infrared spectroscopic characterization and optimization of Pb(II) biosorption by fish (*Labeo rohita*) scales, J. Hazard. Mater. 156 (2008) 64–73.
- [16] A. Kapoor, T. Viraraghavan, Fungal biosorption an alternative treatment option for heavy metal bearing wastewaters. A review, Bioresour. Technol. 53 (1995) 195–206.
- [17] V.K. Gupta, A.K. Shrivastava, N. Jain, Biosorption of chromium(VI) from aqueous solutions by green algae *spirogyra* species, Water Res. 35 (2001) 4079–4085.
- [18] S.K. Lagergren, About the theory of so called adsorption of soluble substances, Kungliga Svenska Vetenskapsakademins Handlingar 24 (1898) 1–39.
- [19] Y.S. Ho, G. Mckay, The kinetics of sorption of divalent metal ions onto sphagnum moss peat, Water Res. 34 (2000) 736–742.
- [20] W.J. Weber, J.C. Morris, Kinetics of adsorption on carbon from solution, J. Sanitary Eng. 89 (1963) 31–60.
- [21] S.J. Allen, G. Mckay, K.Y.H. Khader, Intraparticle diffusion of basic dye during adsorption on to Sphagnum peat, Environ. Pollut. 56 (1989) 39–50.
- [22] Y. Khambhaty, K. Mody, S. Basha, B. Jha, Kinetics, equilibrium and thermodynamic studies on biosorption of hexavalent chromium by dead fungal biomass of marine *Aspergillus niger*, Chem. Eng. J. 145 (2009) 489–495.
- [23] I. Langmuir, The constitution and fundamental properties of solids and liquids, J. Am. Chem. Soc. 38 (1916) 2221–2295.
- [24] H.M.F. Freundlich, Uber die adsorption in lasugen, J. Phys. Chem. 57 (1906) 385–470.
- [25] J.P. Hobson, Physical adsorption isotherms extending from ultrahigh vacuum to vapor pressure, J. Phys. Chem. 73 (1969) 2720–2727.
- [26] S.K. Das, A.K. Guha, Biosorption of chromium by *Termitomyces clypeatus*, Colloids Surf. B: Biointerfaces 60 (2007) 4–57.
- [27] J.F. Villanueva-Espinosa, M. Hernandez-Esparza, F.A. Ruiz-Trevino, Adsorptive properties of fish scales of *Oreochromis niloticus* (Mojorra Tilapia) for metallic ion removal from waste water, Ind. Eng. Chem. Res. 40 (2001) 3563–3569.